Luis Alvarez[1]
Professor
e-mail: alvar@pumas.iingen.unam.mx
Instituto de Ingeniería Universidad Nacional Autónoma de México, 04510 Coyoacán DF, México

Jingang Yi[2]
e-mail: jgyi@me.berkeley.edu

Roberto Horowitz
Professor
e-mail: horowitz@me.berkeley.edu

Department of Mechanical Engineering, University of California, Berkeley, CA 94720-1740

Luis Olmos
Graduate Student
e-mail: luiso10@yahoo.com
Instituto de Ingeniería Universidad Nacional Autónoma de México, 04510 Coyoacán DF, México

Dynamic Friction Model-Based Tire-Road Friction Estimation and Emergency Braking Control

An adaptive control scheme for emergency braking of vehicles is designed based on a LuGre dynamic model for the tire-road friction. The wheel angular speed and longitudinal vehicle acceleration information are used to design a fast convergence observer to estimate the vehicle velocity and the internal state of the friction model. The unknown parameters of the dynamic friction model are estimated through a parameter adaptation law. A Lyapunov-based state estimator and a stabilizing braking controller are designed to achieve near to maximum braking capability of the vehicle. Underestimation of the maximum friction coefficient, a very desirable feature from the perspective of safety, is guaranteed by a proper choice of adaptation gains and initial values of the estimated friction parameters. [DOI: 10.1115/1.1870036]

Keywords: Automotive Control, Adaptive Control, Nonlinear Observers

1 Introduction

In recent years, important research has been undertaken to investigate safety in both manual traffic and automated highway systems (AHS) when highway densities are significantly increased [1–3]. One specific issue that greatly impacts overall safety is the influence of the tire-road interaction on the braking capabilities of vehicles during emergency braking manuevers, which are crucial to preserve safety in AHS [4].

A precise knowledge of the tire-road friction characteristics is important not only from the perspective of emergency braking. It also provides key information regarding safe spacing policies that are useful at vehicle and traffic management centers levels. In both cases, the provided information allows to improve safety. However, tire-road friction characteristics are difficult to estimate due to model complexities and variation of physical conditions.

Research in tire-road friction modeling and estimation for individual vehicles is abundant. The pseudostatic model given in [5], known as the "magic formula," gives a good approximation to experimental results and is widely used in automotive research and industries. However, this model has a complex analytical structure and its parameters are difficult to identify. For these reasons the magic formula is more used for simulation than for control purposes. In [6,7], identifiable pseudostatic parametric friction models are presented. Although the parameters in these models lack direct physical interpretation, they can be identified through on-line adaptation.

Recently, dynamic friction models, such as the one presented in [8], were introduced to capture the friction phenomenon more accurately. These dynamic friction models can reproduce observed behavior that static models, as the magic formula [5], cannot capture: hysteretic cycles and Stribeck effect, among others. Their parameters can be related with materials properties, such as stiffness and viscous damping, and therefore their effects are easier to analyze.

In [9] a *LuGre* model, which is a first-order dynamic friction model, was introduced to replicate the tire-road interface. This model was modified in [10] to include one parameter to represent different road conditions. An adaptation law was proposed to estimate this parameter during vehicle traction. In [11] an adaptive emergency braking controller was designed based on a similar dynamic friction model.

The goal of this paper is to extend the work of [11], where the authors assumed that only one parameter in the LuGre dynamic friction model was unknown to design a controller-observer for emergency braking control. The results in [11] showed the problem of slow convergence of the estimated vehicle velocity and relative velocity due to the structure of the vehicle-tire system dynamics. In this paper most of the tire-road model parameters are assumed unknown. In addition, in order to overcome the slow convergence problem in the estimator, a parameter adaptation law that uses measurements of both angular velocity of the wheel and vehicle longitudinal acceleration is designed. Moreover, the adaptation scheme proposed in this paper achieves underestimation of the maximum friction coefficient, under the proper choice of the parameter adaptation gains and initial conditions of the estimated parameters. This is a very desirable feature from the safety point of view [1,7].

Although this paper is constrained to longitudinal control of emergency braking, the knowledge of the tire-road model parameters is also important when lateral control comes into play. The application of this dynamic friction model to three-dimensional tire-road behavior has been proposed in [12].

The paper is divided into six sections. Section 2 describes the vehicle system dynamics. A controller for emergency braking manuevers that combines an adaptive algorithm with observers for the velocity and the friction internal state is presented in Sec. 3. A Lyapunov-based stability analysis for the observers and parameter adaptation law is also presented in this section. Section 4 analyzes the conditions to achieve underestimation of the maximum fric-

[1]Corresponding author.
[2]Currently with Lam Research Corporation.

Contributed by the Dynamic Systems, Measurement, and Control Division of THE AMERICAN SOCIETY OF MECHANICAL ENGINEERS for publication in the ASME JOURNAL OF DYNAMIC SYSTEMS, MEASUREMENT, AND CONTROL. Manuscript received by the ASME Dynamic Systems and Control Division January 17, 2003; final revision, June 21, 2004. Review conducted by: A. Alleyne.

tion coefficient. Simulation results for this estimation and control scheme are presented in Sec. 5. Finally, Sec. 6 contains concluding remarks and directions for future work.

2 System Dynamics

This paper considers only the longitudinal dynamics of the vehicle. It is assumed that the four wheels of the vehicle apply the same braking force. For simplicity, it is also assumed that the road has no slope and that the weight of the vehicle is distributed evenly among the four wheels. A quarter vehicle model[3] that includes a modified lumped LuGre friction model is as follows [11]:

$$\dot{z} = v_r - \frac{\sigma_0 |v_r|}{h(v_r)} z = v_r - \sigma_0 f(v_r) z \tag{1a}$$

$$J\dot{\omega} = rF_x - u_\tau \tag{1b}$$

$$m\dot{v} = -4F_x - F_a \tag{1c}$$

where z is the friction internal state, $v_r = v - r\omega$ is the relative velocity, r the wheel radius, $h(v_r) = \mu_c + (\mu_s - \mu_c)e^{-|v_r/v_s|^{1/2}}$, $f(v_r) = |v_r|/h(v_r)$, μ_s is the normalized static friction coefficient, μ_c is the normalized Coulomb friction coefficient, v_s is the Stribeck relative velocity, u_τ is the traction-braking torque, F_x the traction-braking force given by the tire-road contact, F_a the aerodynamic force, m the vehicle mass, J the tire rotational inertia, and the parameter σ_0 is the rubber longitudinal stiffness. The model in Eq. (3) has been modified by [13] to consider the case when the friction force in the contact patch is not evenly distributed. This leads to include a "convective" term in Eq. (3). For simplicity, in this paper, the friction force is assumed uniformly distributed in the contact patch.

The braking force F_x is given by

$$F_x = F_n(\sigma_0 z + \sigma_1 \dot{z} + \sigma_2 v_r) \tag{2}$$

where σ_1 is the rubber longitudinal damping, σ_2 is the viscous relative damping and the normal force $F_n = mg/4$, if vehicle mass is uniformly distributed among the four tires. It is possible to use another factor, to consider that during braking there is a shift in the load that will increase the normal force in the front tires. According to [14], the aerodynamic force can be modeled as

$$F_a = C_{av} v^2$$

where C_{av} is he aerodynamic coefficient.

Substituting the above equation into Eq. (1*c*) and considering $v_r = v - r\omega$ as the state variable, Eqs. (1*b*) and (1*c*) can be rewritten as

$$\dot{v} = -c\mu - dv^2 \tag{3a}$$

$$\dot{v}_r = -(a + c)\mu - dv^2 + eK_b P_b \tag{3b}$$

with $a = r^2 mg/4J$, $c = g$, $d = C_{av}/m$ and $e = r/J$. As suggested in [15], the braking torque is approximated by $u_b = K_b P_b$, where K_b is an overall braking system gain and P_b the controlled master cylinder pressure.

3 Controller-Observer Design

3.1 Velocity Observer. Assuming that the wheel angular velocity and the vehicle longitudinal acceleration are known,[4] the instantaneous value of μ can be derived from Eq. (1*b*). It is possible to propose the following observer for the vehicle velocity

$$\dot{\hat{v}} = -c\mu - d\hat{v}^2 + L\tilde{y}_2 \tag{4}$$

where $\tilde{y}_2 := \dot{v} - \dot{\hat{v}} = -d\tilde{v}(v + \hat{v})$ with $\dot{\hat{v}} := -c\mu - d\hat{v}^2$.

The velocity estimation error dynamics are

$$\dot{\tilde{v}} = -d\tilde{v}(v + \hat{v})(1 - L) \tag{5}$$

Define the Lyapunov candidate function

$$W_1 = \tfrac{1}{2}\tilde{v}^2 \tag{6}$$

Its time derivative is

$$\dot{W}_1 = \tilde{v}\dot{\tilde{v}} = -d\tilde{v}^2(v + \hat{v})(1 - L) \leqslant 0$$

Introduce the following lemma

Lemma 1: *Assume* $L < 0$, *then* $\tilde{v}(0) < 0 \Rightarrow \tilde{v}(t) < 0$, $\forall t \geqslant 0$ *or* $\tilde{v}(0) > 0 \Rightarrow \tilde{v}(t) > 0$, $\forall t \geqslant 0$.

Proof: For any given value of v and $\hat{v}$ the solution to Eq. (5) is of the form

$$\tilde{v}(t) = \tilde{v}(0)e^{-(1-L)\int_0^t d(v+\hat{v})d\tau} \tag{7}$$

This term will never change sign, therefore, if $\tilde{v}(0) < 0 \Rightarrow \tilde{v}(t) < 0$, $\forall t \geqslant 0$ or if $\tilde{v}(0) > 0 \Rightarrow \tilde{v}(t) > 0$, $\forall t \geqslant 0$. ■

Remark 1 Lemma 1 implies $\dot{W}_1 < 0$ and asymptotic stability of $\tilde{v} = 0$ follows. Moreover, if the observer gain $|L|$ is chosen large enough, the estimated vehicle velocity $\hat{v}$ converges quickly to the true value v.

The error dynamics of this velocity observer depends only on the longitudinal velocity. In this sense it is different from other observers reported in the literature that used both longitudinal acceleration and wheel angular velocity measurements.

3.2 Internal State Observer and Adaptive Parameters Estimation. First note that substituting Eq. (1*a*) into Eq. (2) yields

$$\mu = \sigma_0 z + \sigma_1[v_r - \sigma_0 f(v_r)z] - \sigma_2 v_r = \sigma_0 z - \sigma_3 f(v_r)z + \sigma_4 v_r \tag{8}$$

where $\sigma_3 = \sigma_0\sigma_1$, $\sigma_4 = \sigma_1 - \sigma_2$ and $f(v_r) = |v_r|/h(v_r)$. This expression is linear in the parameters σ_0, σ_3 and σ_4, i.e.,

$$\mu = [z - f(v_r)z \; v_r]\begin{bmatrix}\sigma_0 \\ \sigma_3 \\ \sigma_4\end{bmatrix} = \mathbf{U}\Theta \tag{9}$$

where $\mathbf{U} := [z - f(v_r)z \; v_r]$ and $\Theta := [\sigma_0 \sigma_3 \sigma_4]^T$.

Propose the following observer for the internal state z

$$\dot{\hat{z}} = \hat{v}_r - \hat{\sigma}_0 f(\hat{v}_r)\hat{z} \tag{10}$$

and a gradient-type parameter adaptation law

$$\dot{\hat{\Theta}} = -\Gamma \hat{\mathbf{U}}^T \tilde{\mu} \tag{11}$$

where $\Gamma = \mathrm{diag}(\gamma_0, \gamma_3, \gamma_4) > 0$ is a diagonal matrix of adaptation gains, $\hat{\mathbf{U}}$ is the regressor in Eq. (9) evaluated at the estimated quantities, i.e.,

$$\hat{\mathbf{U}} = [\hat{z} - f(\hat{v}_r)\hat{z} \; \hat{v}_r]$$

and $\tilde{\mu}$ is defined by

$$\tilde{\mu} = \mathbf{U}\Theta - \hat{\mathbf{U}}\hat{\Theta} = \hat{\mathbf{U}}\tilde{\Theta} + \tilde{\mathbf{U}}\Theta \tag{12}$$

with $\tilde{\mathbf{U}} = \mathbf{U} - \hat{\mathbf{U}}$. $\tilde{\mu} = \mu - \hat{\mu}$ is defined as the estimation error on the friction coefficient. Note that the friction coefficient μ is calculated by the dynamics (1*b*) as

$$\mu = -\frac{J\dot{\omega} + eK_b P_b}{p} \tag{13}$$

with $p = mgr/4$ and assuming that the angular acceleration and the

[3] This simplified model is common in the tire-road friction literature.

[4] This is a reasonable assumption as most modern vehicles already have wheel angular velocity measurements, and solid-state accelerometers are cheap and easy to install.

braking pressure can be measured.[5]

Rearrange Eq. (12) to obtain

$$\tilde{\mu} = [\hat{z} - f(\hat{v}_r)\hat{z}\ \hat{v}_r]\begin{bmatrix}\tilde{\sigma}_0\\ \tilde{\sigma}_3\\ \tilde{\sigma}_4\end{bmatrix} + [\tilde{z} - f(v_r)z + f(\hat{v}_r)\hat{z}\ \tilde{v}_r]\begin{bmatrix}\sigma_0\\ \sigma_3\\ \sigma_4\end{bmatrix} = [\sigma_0 - \sigma_3 f(v_r)]\tilde{z} + \hat{z}\tilde{\sigma}_0 - f(\hat{v}_r)\hat{z}\tilde{\sigma}_3 + \hat{v}_r\tilde{\sigma}_4 + \sigma_4\tilde{v}_r - \sigma_3\hat{z}[f(v_r) - f(\hat{v}_r)] \tag{14}$$

The term $f(v_r) - f(\hat{v}_r)$ can be expanded in a Taylor series about v_r. This yields

$$f(v_r) - f(\hat{v}_r) = \frac{df(v_r)}{dv_r}\tilde{v}_r = \frac{df(v_r)}{dv_r}\tilde{v} \tag{15}$$

where the last expression was derived using the fact that $v_r = v - r\omega$ and $\hat{v}_r = \hat{v} - r\omega$, therefore, $\tilde{v}_r = v_r - \hat{v}_r = \tilde{v}$. Substituting Eq. (15) into Eq. (14)

$$\tilde{\mu} = [\sigma_0 - \sigma_3 f(v_r)]\tilde{z} + \hat{z}\tilde{\sigma}_0 - f(\hat{v}_r)\hat{z}\tilde{\sigma}_3 + \hat{v}_r\tilde{\sigma}_4 + [\sigma_4 - \sigma_3\hat{z}f'(v_r)]\tilde{v} \tag{16}$$

with $f'(v_r) = df(v_r)/dv_r$.[6]

The error dynamics of $\tilde{z}$ from Eqs. (1*a*) and (10) are given by

$$\dot{\tilde{z}} = [1 - \sigma_0 f'(v_r)\hat{z}]\tilde{v} - \sigma_0 f(v_r)\tilde{z} - f(\hat{v}_r)\hat{z}\tilde{\sigma}_0 \tag{17}$$

3.3 Controller Design. In this paper, the LuGre dynamic tire-road friction model is used to estimate a target maximum slip λ_m for the emergency braking maneuver. To calculate this value of λ_m it is necessary to obtain an equivalent pseudostatic solution for the dynamic friction model such that for a given velocity it will be possible to locate the relative velocity at which maximum coefficient of friction is attained. Assuming that vehicle velocity v is constant and that normal force is uniformly distributed on a rectangular tire-road contact patch, then a distributed LuGre tire-road friction model can be solved to obtain the following pseudostatic relationship between μ and $\lambda = v_r/v$

$$\mu(\lambda, v_r, \Theta) = h(v_r)\left\{1 + 2\gamma\frac{h(v_r)}{\sigma_0 l|\eta|}(e^{-[(\sigma_0 l|\eta|)/2h(v_r)]} - 1)\right\} + \sigma_2 v_r,$$

$$\eta = \frac{v_r}{r\omega} = \frac{\lambda}{1-\lambda}, \quad \gamma = 1 - \frac{\sigma_1|\eta|}{r\omega h(v_r)} \tag{18}$$

where l is the length of the tire-road contact patch. Details to obtain this equivalent pseudostatic solution can be found in [11,16]. The value of λ_m is obtained from

$$\lambda_m = \underset{\lambda}{\text{argmax}}\{\mu(\lambda, v_r, \Theta)\}$$

To continue with the controller design, it is necessary to set the value for the pressure of the master cylinder P_b; for that purpose define

$$\tilde{s} = \hat{v}_r - \hat{\lambda}_m\hat{v} = \hat{v}(1 - \hat{\lambda}_m) - r\omega \tag{19}$$

as the desired relative velocity for the emergency braking maneuver. In this expression $\hat{v}_r = \hat{v}_r - r\omega$ and $\hat{\lambda}_m$ is the estimated value of λ_m based on the current estimation of $\hat{v}$, i.e., $\hat{\lambda}_m = \arg\max_{\lambda}\{\mu(\hat{\lambda}, v_r, \hat{\Theta})\}$. Taking the time derivative of Eq. (19)

$$\dot{\tilde{s}} = \dot{\hat{v}}(1 - \hat{\lambda}_m) - r\dot{\omega} - \hat{v}\dot{\hat{\lambda}}_m = \dot{\hat{v}}(1 - \hat{\lambda}_m) - \frac{rf}{J}\mu + \frac{reK_bP_b}{J} - \hat{v}\frac{\partial\hat{\lambda}_m}{\partial\hat{v}}\dot{\hat{v}} - \hat{v}\frac{\partial\hat{\lambda}_m}{\partial\omega}\dot{\omega} \tag{20}$$

The partial derivatives of λ_m can be calculated numerically. Choosing

$$P_b = \frac{J}{reK_b}\left[-\dot{\hat{v}}(1 - \hat{\lambda}_m) + \frac{rf}{J}\mu + \hat{v}\frac{\partial\hat{\lambda}_m}{\partial\hat{v}}\dot{\hat{v}} + \hat{v}\frac{\partial\hat{\lambda}_m}{\partial\omega}\dot{\omega} - \zeta\tilde{s}\right] \tag{21}$$

where $\zeta > 0$ is a gain and substituting in Eq. (20) gives

$$\dot{\tilde{s}} = -\zeta\tilde{s} \tag{22}$$

Define the following Lyapunov function candidate

$$W_4 = \tfrac{1}{2}\tilde{s}^2 \tag{23}$$

Taking the time derivative of Eq. (23) and using Eq. (22)

$$\dot{W}_4 = -\zeta\tilde{s}^2 \leqslant 0 \tag{24}$$

The asymptotic stability of $\tilde{s} = 0$ follows.

3.4 Combined Stability Analysis. Propose, in addition to Eq. (6), the following set of Lyapunov function candidates

$$W_2 = \tfrac{1}{2}\tilde{z}^2 \tag{25}$$

$$W_3 = \tfrac{1}{2}\tilde{\Theta}^T\Gamma^{-1}\tilde{\Theta} \tag{26}$$

and define now the composite Lyapunov function candidate

$$W = W_1 + W_2 + W_3 = \sum_{i=1}^{3} W_i \tag{27}$$

The time derivative of Eq. (27) can be written as

$$\dot{W} = \tilde{v}\dot{\tilde{v}} + \tilde{z}\dot{\tilde{z}} + \tilde{\Theta}^T\Gamma^{-1}\dot{\tilde{\Theta}} \tag{28}$$

Using the observer error dynamics and parameter adaptation law in Eqs. (5), (17), and (11), Eq. (28) becomes

$$\dot{W} = -d(v + \hat{v})(1 - L)\tilde{v}^2 + \tilde{z}[(1 - \sigma_0 f'(v_r)\hat{z})\tilde{v} - \sigma_0 f(v_r)\tilde{z} - f(\hat{v}_r)\hat{z}\tilde{\sigma}_0] - (\tilde{\Theta}^T\hat{\mathbf{U}}^T\hat{\mathbf{U}}\tilde{\Theta} + \tilde{\Theta}^T\hat{\mathbf{U}}^T\tilde{\mathbf{U}}\Theta) \tag{29}$$

The term $\tilde{\mathbf{U}}$ can be expressed as

$$\tilde{\mathbf{U}} = [0\ \ -f'(v_r)\hat{z}\ \ 1]\tilde{v} + [1\ \ -f(v_r)\ \ 0]\tilde{z} = \mathbf{U}_1\tilde{v} + \mathbf{U}_2\tilde{z} \tag{30}$$

where $\mathbf{U}_1 = [0\ -f'(v_r)\hat{z}\ 1]$ and $\mathbf{U}_2 = [1\ -f(v_r)\ 0]$. Using Eq. (30), Eq. (29) can be written as a quadratic form

$$\dot{W} = -[\tilde{\Theta}\tilde{z}\tilde{v}]\begin{bmatrix}\hat{\mathbf{U}}^T\hat{\mathbf{U}} & \hat{\mathbf{U}}^T\mathbf{U}_2\Theta & \hat{\mathbf{U}}^T\mathbf{U}_1\Theta\\ \mathbf{U}_3 & \sigma_0 f(v_r) & -(1 - \sigma_0 f'(v_r)\hat{z})\\ \mathbf{0} & 0 & d(1 - L)(v + \hat{v})\end{bmatrix}\begin{bmatrix}\tilde{\Theta}\\ \tilde{z}\\ \tilde{v}\end{bmatrix} = -\Phi^T\mathbf{M}\Phi \tag{31}$$

where $\Phi = [\tilde{\Theta}\ \tilde{z}\ \tilde{v}]^T = [\tilde{\sigma}_0\ \tilde{\sigma}_4\ \tilde{\sigma}_4\ \tilde{z}\ \tilde{v}]^T$, $\mathbf{U}_3 = [f(\hat{v}_r)\hat{z}\ 0\ 0]$ and

$$\mathbf{M} = \begin{bmatrix}\hat{z}^2 & -\hat{z}^2 f(\hat{v}_r) & \hat{z}\hat{v}_r & w_1\hat{z} & w_2\hat{z}\\ -\hat{z}^2 f(\hat{v}_r) & \hat{z}^2 f^2(\hat{v}_r) & -\hat{z}f(\hat{v}_r)\hat{v}_r & -w_1\hat{z}f(\hat{v}_r) & -w_2\hat{z}f(\hat{v}_r)\\ \hat{z}\hat{v}_r & -\hat{z}f(\hat{v}_r)\hat{v}_r & \hat{v}_r^2 & w_1\hat{v}_r & w_2\hat{v}_r\\ \hat{z}f(\hat{v}_r) & 0 & 0 & \sigma_0 f(v_r) & -w_3\\ 0 & 0 & 0 & 0 & w_4\end{bmatrix}$$

with $w_1 = \sigma_0 - \sigma_3 f(v_r)$, $w_2 = \sigma_4 - \sigma_3 f'(v_r)\hat{z}$, $w_3 = 1 - \sigma_0 f'(v_r)\hat{z}$, and $w_4 = d(1-L)(v+\hat{v})$.

Note that

[5]Angular acceleration can be calculated from wheel angular velocity measurements, while the master cylinder braking pressure can be obtained from the brake actuator.

[6]It should be noted that the function $f(v_r)$ is not differentiable with respect to v_r when $v_r = 0$. It is assumed, however, that during emergency braking the sign of v_r does not change.

$$\mathbf{M} = \frac{\mathbf{M}+\mathbf{M}^T}{2} + \frac{\mathbf{M}-\mathbf{M}^T}{2} = \mathbf{M}_1 + \mathbf{M}_2$$

where $\mathbf{M}_1 = \mathbf{M}_1^T = (\mathbf{M}+\mathbf{M}^T)/2$ is a symmetric matrix and $\mathbf{M}_2 = -\mathbf{M}_2^T = (\mathbf{M}-\mathbf{M}^T)/2$ is a skew-symmetric matrix. Thus, Eq. (31) becomes

$$\dot{W} = -\Phi^T\mathbf{M}_1\Phi - \Phi^T\mathbf{M}_2\Phi = -\Phi^T\mathbf{M}_1\Phi$$

The last equality comes from the fact that $\Phi^T\mathbf{M}_2\Phi = 0$. It is direct to show that the symmetric matrix

$$\mathbf{M}_1 = \begin{bmatrix} \hat{z}^2 & -\hat{z}^2 f(\hat{v}_r) & \hat{z}\hat{v}_r & \frac{1}{2}\hat{z}(w_1 + f(\hat{v}_r)) & \frac{1}{2}\hat{z}w_2 \\ -\hat{z}^2 f(\hat{v}_r) & \hat{z}^2 f^2(\hat{v}_r) & -\hat{z}f(\hat{v}_r)\hat{v}_r & -\frac{1}{2}\hat{z}w_1 f(\hat{v}_r) & -\frac{1}{2}w_2\hat{z}f(\hat{v}_r) \\ \hat{z}\hat{v}_r & -\hat{z}f(\hat{v}_r)\hat{v}_r & \hat{v}_r^2 & \frac{1}{2}w_1\hat{v}_r & \frac{1}{2}w_2\hat{v}_r \\ \frac{1}{2}\hat{z}(w_1 + f(\hat{v}_r)) & -\frac{1}{2}\hat{z}w_1 f(\hat{v}_r) & \frac{1}{2}w_1\hat{v}_r & \sigma_0 f(v_r) & -\frac{1}{2}w_3 \\ \frac{1}{2}\hat{z}w_2 & -\frac{1}{2}w_2\hat{z}f(\hat{v}_r) & \frac{1}{2}w_2\hat{v}_r & -\frac{1}{2}w_3 & w_4 \end{bmatrix} \geqslant 0 \tag{32}$$

by the fact that

$$\det \mathbf{M}_1(1,1) = \hat{z}^2 > 0, \quad \det \mathbf{M}_1(1{:}j, 1{:}j) = 0, \quad \text{for } j = 2,3,4,5$$

From Eq. (32) it is known that

$$\dot{W} = -\Phi^T M_1 \Phi \leqslant 0$$

which indicates that Eq. (31) is negative semi-definite. The stability of $\tilde{v}=0$, $\tilde{z}=0$, and $\tilde{\Theta}=\mathbf{0}$ follows. Using Barbalat's Lemma it is possible to show that $\lim_{t\to\infty}\tilde{v}(t)=0$. Convergence of $\tilde{z}=0$ and $\tilde{\Theta}=\mathbf{0}$ cannot be guaranteed if there is no persistence of excitation. Using the fact that $\tilde{v}=0$, in this case the equilibria that are reached satisfy

$$\tilde{\sigma}_0\hat{z}\left(1 - \frac{w_1}{\sigma_0}\right) - \hat{z}f(v_r)\tilde{\sigma}_3 + \hat{v}_r\tilde{\sigma}_4 = 0 \tag{33}$$

$$\tilde{z} + \frac{\hat{z}}{\sigma_0}\tilde{\sigma}_0 = 0 \tag{34}$$

Remark 2 In the above combined stability analysis the Lyapunov candidate W_4 introduced for the controller design controller was not included because the controlled target error $\tilde{s}$ given by (19) is decoupled with the observer and parameter adaptation errors $\tilde{\Theta}, \tilde{z}$, and $\tilde{v}$. Therefore, the stability of the controller is analyzed separately to the observers and the parameter estimators.

4 Underestimation of Friction Coefficient

A very desirable feature to be attained with the observer and adaptive scheme in Eqs. (5), (11), and (17) is the underestimation of the maximum coefficient of friction μ_m. This underestimation provides conservative estimates for the intervehicle distance that will yield safe emergency braking maneuvers.

From Eq. (8) it is clear that

$$\tilde{\sigma}_0(t) \geqslant 0, \quad \tilde{\sigma}_3(t) \leqslant 0, \quad \text{and } \tilde{\sigma}_4(t) \geqslant 0 \tag{35}$$

will produce this desired underestimation property, i.e., $\hat{\mu}_m(t) \leqslant \mu_m(t)$ provided that:

Assumption 1

1. The estimated state variable $\hat{v}$ converge to its true state quickly.
2. The estimated state variable $\hat{z}$ converges quickly.
3. $z \geqslant 0$, $v_r \geqslant 0$ and $f(v_r) \geqslant 0$.

Remark 3 To justify the first condition in Assumption 1, recall the error dynamics of state variable $\tilde{v}$ given by Eqs. (5). By choosing a large observer gain L, the quick convergence of $\hat{v}$ can be guaranteed by Lemma 1. The second condition can be obtained by analyzing the error dynamics of $\tilde{z}$ in Eq. (17). The quick convergence rate of estimated state $\hat{z}$ follows from Eq. (17), and the facts that $\tilde{v}\to 0$, σ_0 is large, and $\hat{z}, \hat{\Theta}$ are bounded. The last condition in Assumption 1 follows directly from the definitions of v_r and $f(v_r)$. It is clear that in this analysis other possible sources of bandwidth constraints of the systems, such as time delays, are not considered. The scheme is designed to be used in vehicles that have direct actuation on the brakes systems. This is necessary if typical human reaction times to emergency situations are to be reduced.

In this section it is assumed that:

Assumption 2

1. $\tilde{\sigma}_0(0) > 0$, $\tilde{\sigma}_3(0) < 0$ and $\tilde{\sigma}_4(0) > 0$.
2. $v(t) \geqslant v_{\min}$, $\forall t \geqslant 0$

Under these assumptions, the structure of the system composed by $\tilde{\sigma}_0, \tilde{\sigma}_3$ and $\tilde{\sigma}_4$ is

$$\begin{bmatrix} \dot{\tilde{\sigma}}_0 \\ \dot{\tilde{\sigma}}_3 \\ \dot{\tilde{\sigma}}_4 \end{bmatrix} = \begin{bmatrix} -\gamma_0\hat{z}^2 & \gamma_0 f(v_r)\hat{z}^2 & -\gamma_0\hat{z}v_r \\ \gamma_3 f(v_r)\hat{z}^2 & -\gamma_3 f^2(v_r)\hat{z}^2 & \gamma_3 f(v_r)\hat{z}v_r \\ -\gamma_4\hat{z}v_r & \gamma_4 f(v_r)\hat{z}v_r & -\gamma_4 v_r^2 \end{bmatrix} \begin{bmatrix} \tilde{\sigma}_0 \\ \tilde{\sigma}_3 \\ \tilde{\sigma}_4 \end{bmatrix} \tag{36}$$

For simplicity, consider the system in Eq. (36) as time invariant in order to find an approximate condition for underestimation of friction coefficient μ. The solution, with initial conditions $\tilde{\sigma}_0(0)$, $\tilde{\sigma}_3(0)$ and $\tilde{\sigma}_4(0)$, is

$$\tilde{\sigma}_0(t) = \frac{1}{\beta}[(\gamma_0\hat{z}^2 e^{-\beta t} + \gamma_3\hat{z}^2 f^2(v_r) + \gamma_4 v_r^2)\tilde{\sigma}_0(0) + (1 - e^{-\beta t})\gamma_0\hat{z}^2 f(v_r)\tilde{\sigma}_3(0) + (1 - e^{-\beta t})\gamma_4 v_r^2\tilde{\sigma}_4(0)] \tag{37a}$$

$$\tilde{\sigma}_3(t) = \frac{1}{\beta}[(1-e^{-\beta t})\gamma_3\hat{z}^2 f(v_r)\tilde{\sigma}_0(0) + (\alpha\gamma_0\hat{z}^2 + \gamma_4 v_r^2 + \gamma_3\hat{z}^2 f^2(v_r)e^{-\beta t})\tilde{\sigma}_3(0) - ((1-e^{-\beta t})\gamma_3\gamma_4 v_r^2/\gamma_0)\tilde{\sigma}_4(0)] \tag{37b}$$

$$\tilde{\sigma}_4(t) = \frac{1}{\beta}[(1-e^{-\beta t})\gamma_0\hat{z}^2\tilde{\sigma}_0(0) - (1-e^{-\beta t})\gamma_0\hat{z}^2 f(v_r)\tilde{\sigma}_3(0) + (\gamma_0\hat{z}^2 + \gamma_3\hat{z}^2 f^2(v_r) + \gamma_4 v_r^2 e^{-\beta t})\tilde{\sigma}_4(0)] \tag{37c}$$

where $\beta = \gamma_0\hat{z}^2 + \gamma_3\hat{z}^2 f^2(v_r) + \gamma_4 v_r^2$.

Lemma 2 *Assume that Lemma 1 and Assumption 2 hold, then there exist gains* γ_0, γ_3, *and* γ_4 *such that if the following conditions are satisfied*

$$\left(\gamma_0 + \gamma_4\frac{v_r^2}{\hat{z}^2}\right)|\tilde{\sigma}_3(0)| \geq \gamma_3 f(v_r)\tilde{\sigma}_0(0) \geq \gamma_0|\tilde{\sigma}_3(0)| \tag{38}$$

then $\tilde{\sigma}_0(t) \geq 0$, $\tilde{\sigma}_3(t) \leq 0$ *and* $\tilde{\sigma}_4(t) \geq 0$, $\forall t \geq 0$.

Proof: First assume that t is close to 0, then the evolution of $\tilde{\sigma}_0(t), \tilde{\sigma}_3(t)$ and $\tilde{\sigma}_4(t)$ is dominated by $\tilde{\sigma}_0(0) > 0$, $\tilde{\sigma}_3(0) < 0$ and $\tilde{\sigma}_4(0) > 0$ because the term $(1-e^{-\beta t})$ can be neglected. Now assume the worst possible case, which happens if $t \gg 0$. In this situation for $\tilde{\sigma}_0(t)$ to remain positive, according to Eq. (37*a*), it is necessary that

$$(\gamma_3\hat{z}^2 f^2(v_r) + \gamma_4 v_r^2)\tilde{\sigma}_0(0) + \gamma_4 v_r^2\tilde{\sigma}_4(0) \geq \gamma_0\hat{z}^2 f(v_r)|\tilde{\sigma}_3(0)| \tag{39}$$

Inequality (39) will hold if

$$\gamma_3\hat{z}^2 f(v_r)\tilde{\sigma}_0(0) \geq \gamma_0\hat{z}^2 f(v_r)|\tilde{\sigma}_3(0)| \tag{40}$$

which is precisely the second inequality in Inequality (38). Similarly, according to Eq. (37*b*), for $\tilde{\sigma}_3(t)$ to remain negative it is necessary that

$$(\gamma_0\hat{z}^2 + \gamma_4 v_r^2)|\tilde{\sigma}_3(0)| + \frac{\gamma_3\gamma_4}{\gamma_0}v_r^2\tilde{\sigma}_4(0) \geq \gamma_3\hat{z}^2 f(v_r)\tilde{\sigma}_0(0) \tag{41}$$

Inequality (41) will hold, in turn, if

$$(\gamma_0\hat{z}^2 + \gamma_4 v_r^2)|\tilde{\sigma}_3(0)| \geq \gamma_3\hat{z}^2 f(v_r)\tilde{\sigma}_0(0) \tag{42}$$

which is the first inequality in Inequality (38). According to Eq. (37*c*), $\tilde{\sigma}_4(t)$ will always remain positive. ■

Finally, the main result of this paper is stated in the following theorem.

Theorem 1 *Consider Assumption 2 and Lemmas 1 and 2, then under the observer and adaptation laws in Eqs.* (4), (10), and (11) *the equilibrium* $\tilde{v}=0, \tilde{z}=0$ *and* $\tilde{\Theta}=\mathbf{0}$ *is stable. Moreover, the maximum coefficient of friction* $\mu_{\max}$ *is underestimated and* $\lim_{t\to\infty}\tilde{v}(t)=0$, $\lim_{t\to\infty}\tilde{z}(t)=0$ *and* $\lim_{t\to\infty}\tilde{\Theta}=\mathbf{0}$.

Proof: The choice of $\tilde{z}(0) < 0$, $\tilde{\sigma}_0(0) > 0$, $\tilde{\sigma}_3(0) < 0$ and $\tilde{\sigma}_4(0) > 0$ together with Lemma 2 implies that $\hat{\mathbf{U}}\tilde{\Theta} \geq 0$ and, therefore, that the product $\tilde{\Theta}^T\hat{\mathbf{U}}^T\hat{\mathbf{U}}\tilde{\Theta}$ does not vanish, except when $\tilde{\Theta}=\mathbf{0}$.

Choose Lyapunov function candidate V as

$$W = h_1 W_1 + h_2 W_2 + h_3 W_3 = \sum_{i=1}^{3} h_i W_i$$

with h_1, h_2, and h_3 are positive numbers. The time derivative of V satisfies, similar as (31),

$$\dot{V} = -[\tilde{\Theta}\ \tilde{z}\ \tilde{v}]\begin{bmatrix} h_3\hat{\mathbf{U}}^T\hat{\mathbf{U}} & h_3\hat{\mathbf{U}}^T\mathbf{U}_2\Theta & h_3\hat{\mathbf{U}}^T\mathbf{U}_1\Theta \\ h_2\mathbf{U}_3 & h_2\sigma_0 f(v_r) & -h_2(1-\sigma_0 f'(v_r)\hat{z}) \\ \mathbf{0} & 0 & h_1 d(1-L)(v+\hat{v}) \end{bmatrix}\begin{bmatrix}\tilde{\Theta}\\ \tilde{z}\\ \tilde{v}\end{bmatrix} \tag{43}$$

Equation (43) can be bounded by

$$\dot{V} \leq -[\|\tilde{\Theta}\|\ |\tilde{z}|\ |\tilde{v}|]\begin{bmatrix} h_3\|\hat{\mathbf{U}}^T\hat{\mathbf{U}}\| & h_3\|\hat{\mathbf{U}}^T\mathbf{U}_2\Theta\| & h_3\|\hat{\mathbf{U}}^T\mathbf{U}_1\Theta\| \\ h_2\|\mathbf{U}_3\| & h_2\sigma_0 f(v_r) & -h_2(1-\sigma_0 f'(v_r)\hat{z}) \\ \mathbf{0} & 0 & h_1 d(1-L)(v+\hat{v}) \end{bmatrix} \times \begin{bmatrix}\|\tilde{\Theta}\|\\ |\tilde{z}|\\ |\tilde{v}|\end{bmatrix} = -\tfrac{1}{2}\Psi^T(\mathbf{HS}+\mathbf{S}^T\mathbf{H})\Psi \tag{44}$$

where $\Psi = [\|\tilde{\Theta}\|\ |\tilde{z}|\ |\tilde{v}|]^T$, $\mathbf{H} = \mathrm{diag}\{h_3, h_2, h_1\}$ and

$$\mathbf{S} = \begin{bmatrix} \|\hat{\mathbf{U}}^T\hat{\mathbf{U}}\| & \|\hat{\mathbf{U}}^T\mathbf{U}_2\Theta\| & \|\hat{\mathbf{U}}^T\mathbf{U}_1\Theta\| \\ \|\mathbf{U}_3\| & \sigma_0 f(v_r) & -(1-\sigma_0 f'(v_r)\hat{z}) \\ \mathbf{0} & 0 & d(1-L)(v+\hat{v}) \end{bmatrix} \tag{45}$$

According to [17] a necessary and sufficient condition for the existence of scalar h_1, h_2, and h_3 that will make Eq. (44) negative definite is that the principal minors of the matrix $\mathbf{S}$ are positive definite. The first two minors are proven directly to be positive, the third one, given by

$$d(1-L)(v+\hat{v})\hat{z}^2 f^2(v_r)\sigma_3 \tag{46}$$

will be greater or equal to zero provided that conditions on Lemmas 1 and 2 are satisfied. This proves asymptotic stability and therefore that $\lim_{t\to\infty}\tilde{v}(t)=0$, $\lim_{t\to\infty}\tilde{z}(t)=0$ and $\lim_{t\to\infty}\tilde{\Theta}=\mathbf{0}$.

The underestimation of $\mu_{\max}$ follows directly from Eq. (8) and Lemma 2. ■

5 Simulation Results

In this section, the controller-observer designed in this paper will be tested by simulations. Before doing that, the ability of the LuGre dynamic friction model to describe tire-road frictions forces is illustrated. Figure 1 shows how the LuGre dynamic friction model and the magic formula [5] fit a set of experimental data obtained from [18]. The curve that corresponds to the dynamic friction model was obtained with the pseudostatic solution described by Eq. (18) in Sec. 3. It is clear from Fig. 1 that the two curves are very similar. Other testing results with different experimental data showed consistent fitting behavior.

Emergency braking manuevuers are simulated. They consist of driving a vehicle traveling at a speed of 30 m/s to a complete stop as soon as possible. It is assumed that just before the vehicle executes the emergency braking manuever, the parameters of the dynamic friction model Θ, the friction internal state z, and the vehicle velocity v are unknown. The observer and adaptation law will work simultaneously with the emergency braking control law.

In order to illustrate the underestimation feature of the controller, it is also assumed that signs of $\tilde{\sigma}_0, \tilde{\sigma}_3$, and $\tilde{\sigma}_4$ are known. It is also important to remark that the scenario that is simulated corresponds to the worst possible case during emergency braking manuevers, i.e., that there is no precise knowledge of the parameters at the moment the emergency braking maneuver has to be initiated. In a normal situation, if the observers and parameter adaptation law are already active before the emergency braking, then the state and friction parameters would be properly known, and the controller would achieve near to maximum emergency braking.[7] However, a much more challenging situation occurs if there is a sudden change in the parameters of the tire-road interface and the controller has to adapt them while performing the emergency braking maneuver.

If the parameter adaptation law is being used, for example, to set a proper intervehicle distance based on the current tire-road

[7]The braking force is not maximum because initially the controller does not apply full brakes, that is the optimal value. Instead, it tries to track asymptotically the desired slip given by $\hat{\lambda}_m$.

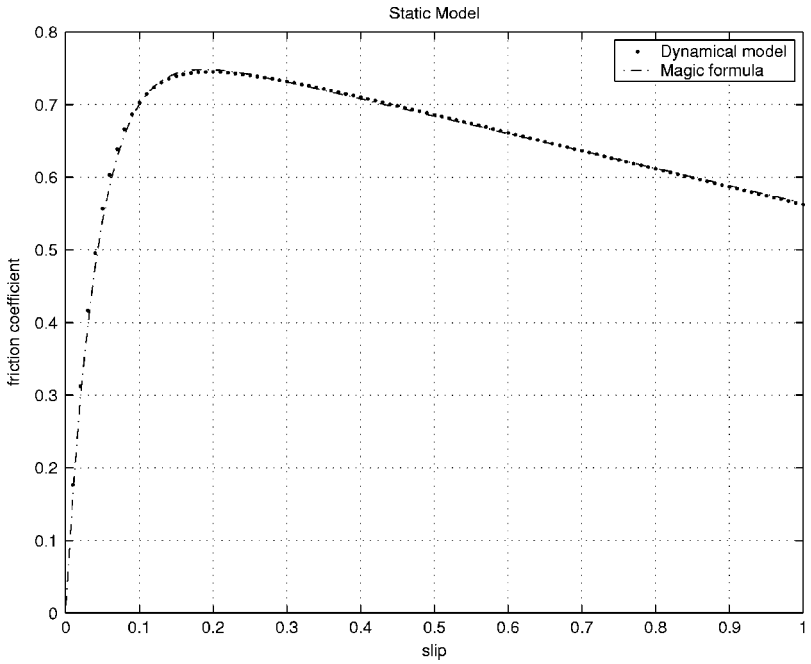

Fig. 1 Comparison between the psedostatic solution of the LuGre dynamic model and the "magic formula" for a braking case

interface, then the controller can guarantee avoidance of rear collisions between vehicles. However, a sudden change on the parameters of this interface can lead to situations where it is not possible to guarantee that a emergency braking would not end in a rear collision. This is the case when the friction coefficient decreases from one point on the road to another. Even in this worst-case scenario, the controller designed in this paper will achieve braking in such a way that in case of a collision, this will happen with the smallest possible velocity. This is the safest behavior one can expect in such a difficult situation.

When a sudden change in the friction coefficient happens, it is convenient to have different sets of possible initial conditions to guarantee underestimation. In this case it is possible to use techniques, such as the one proposed by [19], that allows one to have a quick indication on the type of tire-road interaction.

The nominal data for the simulation are taken from the parameters of the LeSabre cars used in the California PATH program as: $M=1701.0$ Kg $C_{av}=0.3693$ N s^2/m^2, $J=2.603$ Kg m^2,$R=0.323$ m and the brake coefficient $K_b=0.9$. The nominal value for the dynamic friction models was obtained off-line by adjusting a proper set of parameters that fit the data of a pseudostatic friction curve [11]. As mentioned before, it is assumed that measurements of wheel angular velocity and vehicle longitudinal accelera-

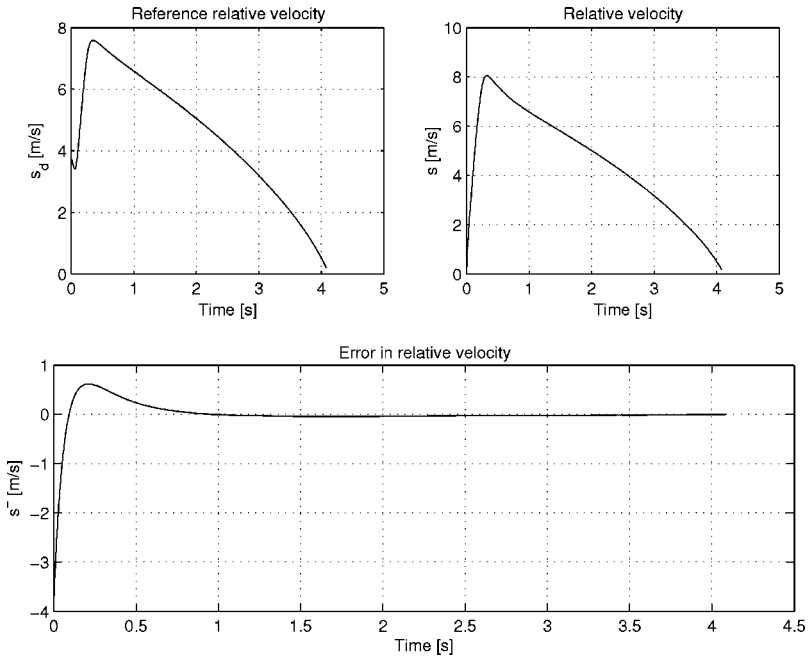

Fig. 2 Dynamic surface $\tilde{s}$

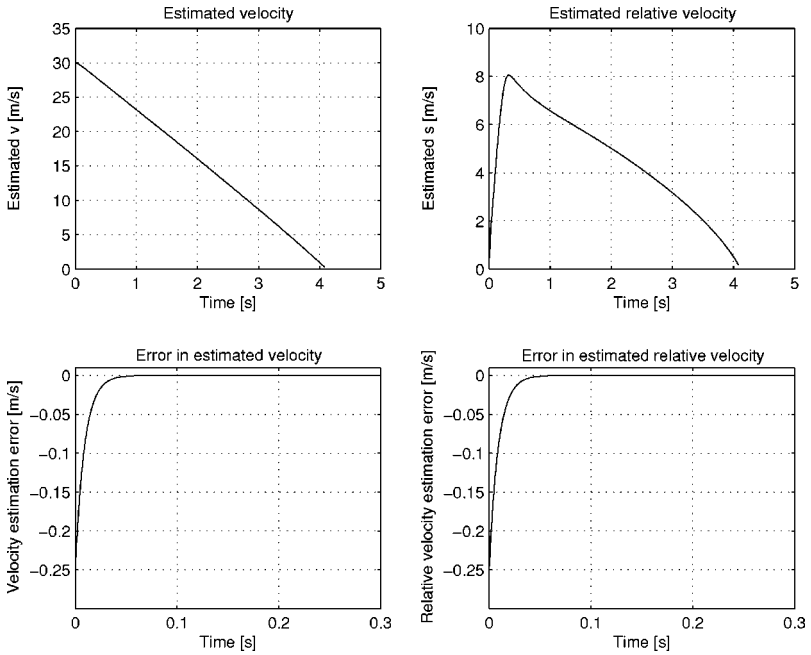

Fig. 3 Estimated velocity ($\hat{v}$) and relative velocity ($\hat{v}_r$)

tion are available. Before attemping an emergency braking maneuver the vehicle is cruising at a constant speed of 30 m/s.

Figure 2 shows the convergence of the dynamic surface $\tilde{s}$ for the emergency braking maneuver. It is clear that the error $\tilde{s}$ converges to zero very fast. Althought the dynamics of the vehicle and the tire-road interface do not allow an instantenous change on the relative velocity, the results in Fig. 2 show that the dynamic surface is first crossed at 0.1 s

Figure 3 illustrates the time evolution of the estimated vehicle velocity and relative velocity. It is shown that both estimated velocities, $\hat{v}$ and $\hat{v}_r$, converge rapidly to their true values. The initial guess for the longitudinal velocity can be obtained from $\hat{v}(0) = wr$.

Figure 4 shows the friction coefficient and braking pressure during the emergency braking maneuver. It is important to realize that there is an increase in the coefficient of friction at the end of the maneuver. This behavior is consistant with other observations in the literature that suggest a velocity dependence in the coefficient of friction [20]. Figure 5 shows the braking acceleration. Magnitude of deceleration increases with time.

The estimated internal friction state z is shown in Fig. 6. Figure 7 illustrates the evolution of the estimated friction parameters $\hat{\Theta}$ when a proper set of initial estimation errors and adaptation gains are chosen. It is clear that when the velocity of the vehicle is above 3 m/s estimated parameters converge. There is a disturbance in the convergence of the parameters at the end of the

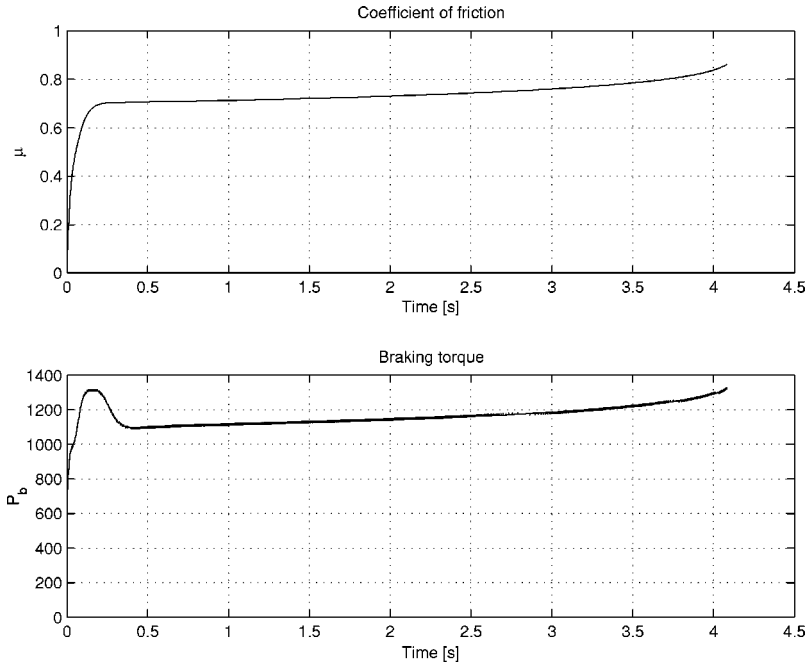

Fig. 4 Friction coefficient μ and braking pressure P_b (KPa)

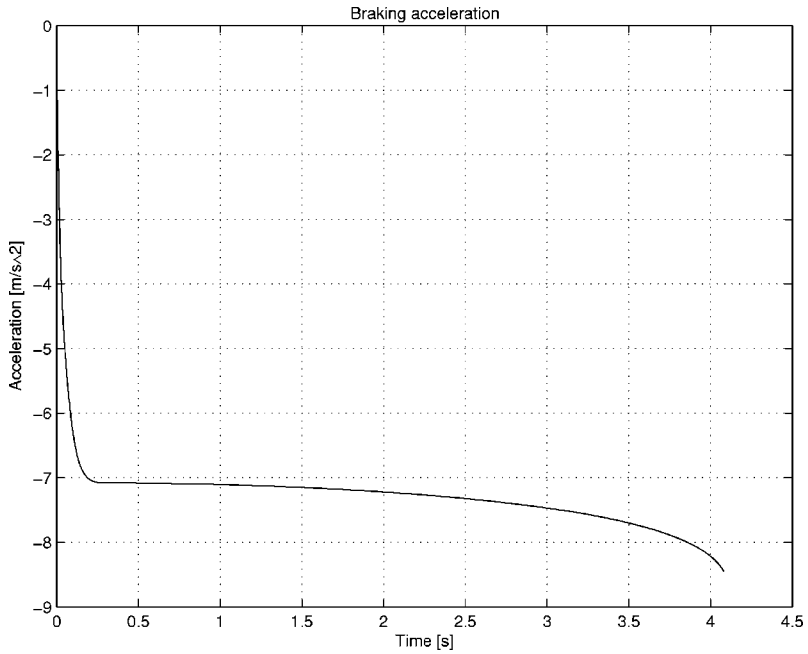

Fig. 5 Braking acceleration

maneuver. In the last 0.5 s the deviations of the estimated parameters result from the "Stribeck effect" that induces a change on the coefficient of friction. It should be noted, from the plot of the error in the coefficient of friction on Fig. 4, that underestimation of maximum friction coefficient occurs at all times.

Figure 8 illustrates parameter evolution in a simulation in which underestimation does not occur. In this case, as Fig. 9 shows, the emergency braking maneuver is still properly completed. However, if the spacing between the vehicle and its leading vehicle is established based on this overestimated maximum friction coefficient, a rear collision may occur. Strategies of coordinated braking, like the one suggested in [1], may prove useful to avoid real collisions even in this case of overestimation. The implementations of this coordinated braking requires, however, some degree of automation in vehicles.

Finally, Fig. 10 shows the evolution of the reference relative velocity, the relative velocity and the dynamic surface $\tilde{s}$ when there is a change in the vehicle mass M of 30% and of the brakes system gain K_b of 10%. It can be noted that even if there is a degradation on performance, the emergency braking maneuver still works properly and shows the robustness of the controller against uncertainties in some of the critical parameters.

Simulation results show that the adaptive controller scheme

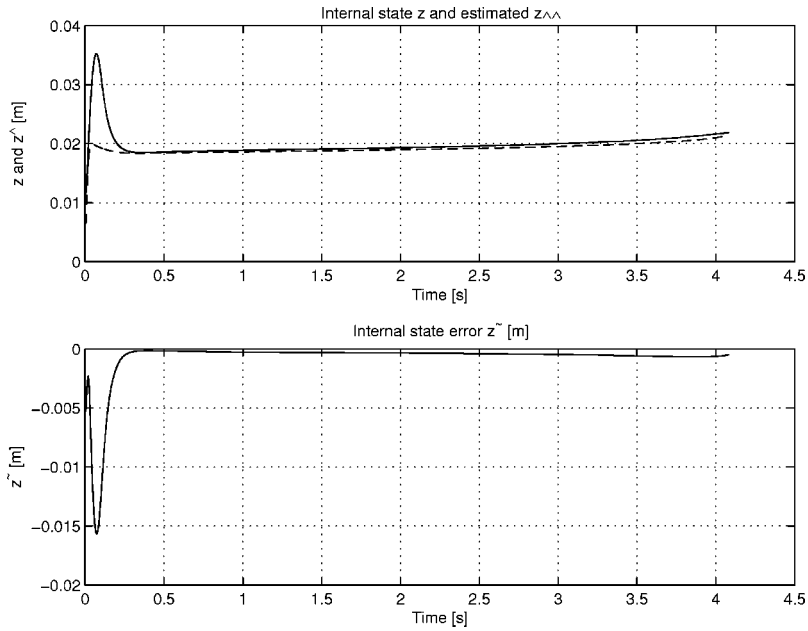

Fig. 6 Internal state (z, dashed), estimated internal state ($\hat{z}$, solid), and estimation error ($\tilde{z}$)

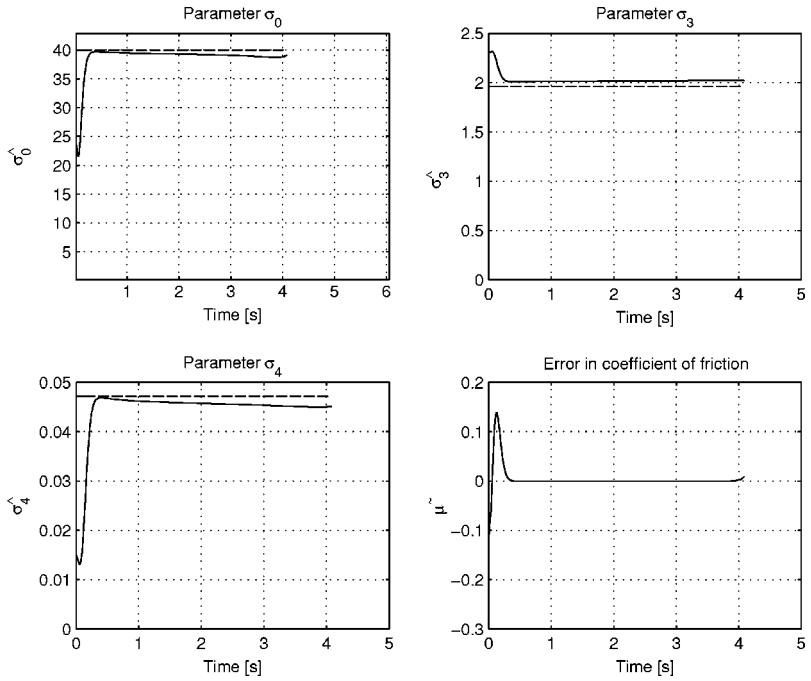

Fig. 7 Adapted parameters; underestimation case, reference value dashed

presented in this paper overcomes the drawback given in [11] by using vehicle longitudinal acceleration in addition to wheel angular velocity. By using these measurements, the lack of observability issue reported in [11] is addressed.

It is important to remark that the simulation results obtained with this dynamic friction approach are not easy to compare to the normal pseudostatic friction curves, as that in Fig. 1. Emergency braking is a dynamic maneuver in which all the states change rapidly. This is very different from the situation that is used in laboratories to produce the pseudostatic friction curves, where the dynamic evolution is controlled and only a limited set of steady-state points are used produce these curves.

It is to expect that the three feedback terms included in the velocity observer, parameter adaptation law, and master cylinder pressure control law will be helpful to compensate errors in the measurement of the instantaneous friction coefficient and of the value for the brakes system gain.

Finally, the simulations are performed in a noise-free scenario.

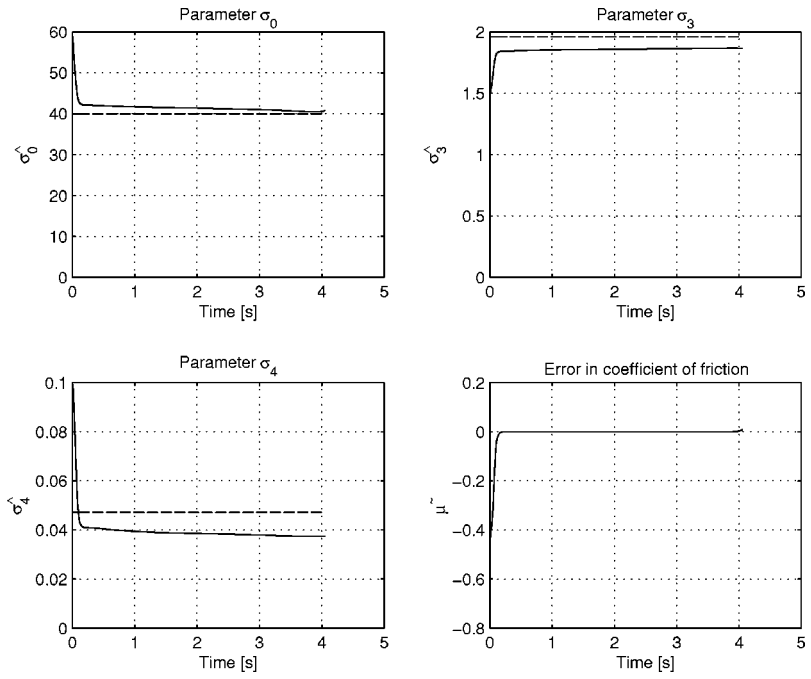

Fig. 8 Adapted parameters; non-underestimation case, reference value dashed

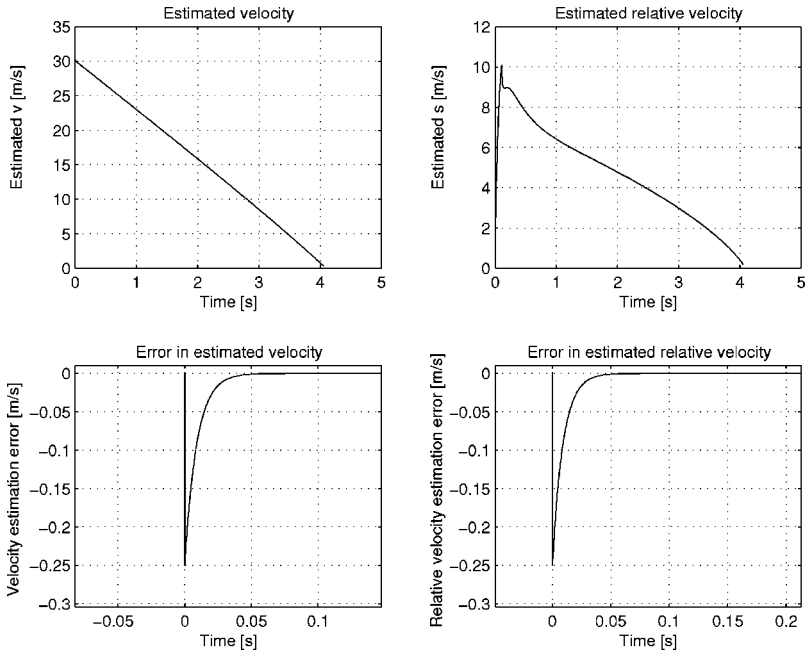

Fig. 9 Estimated of velocity ($\hat{v}$) and relative velocity ($\hat{v}_r$); non-underestimation case

The lack of this noise is a severe disadvantage for the identification process. The exciting signal in this case, the emergency braking trajectory, is a signal that lacks persistence of excitation conditions. Therefore, the results obtained represents a pesimistic scenario.

6 Conclusions

In this paper emergency braking control of vehicles was discussed. Under the assumption that a first-order dynamic friction model appropriately represents the behavior of the tire-road forces, a controller-observer scheme was designed to determine the unknown tire-road model parameters and the nonmeasured system states. It was assumed that measurements of wheel angular velocity and longitudinal acceleration are available, which is a reasonable assumption in modern vehicles. The control law sets the master cylinder pressure in such a way that near-optimum braking was achieved. Stability analysis of the combined controller-observer scheme was presented. The reference trajectory for the maneuver tried to keep maximum friction at all times during the braking process. Moreover, under the proper choice of gains of the parameter adaptation law and initial values of estimated parameters, the proposed scheme was shown to achieve underestimation of the maximum friction coefficient under lack of persistence of excitation. This is a very desirable feature from the

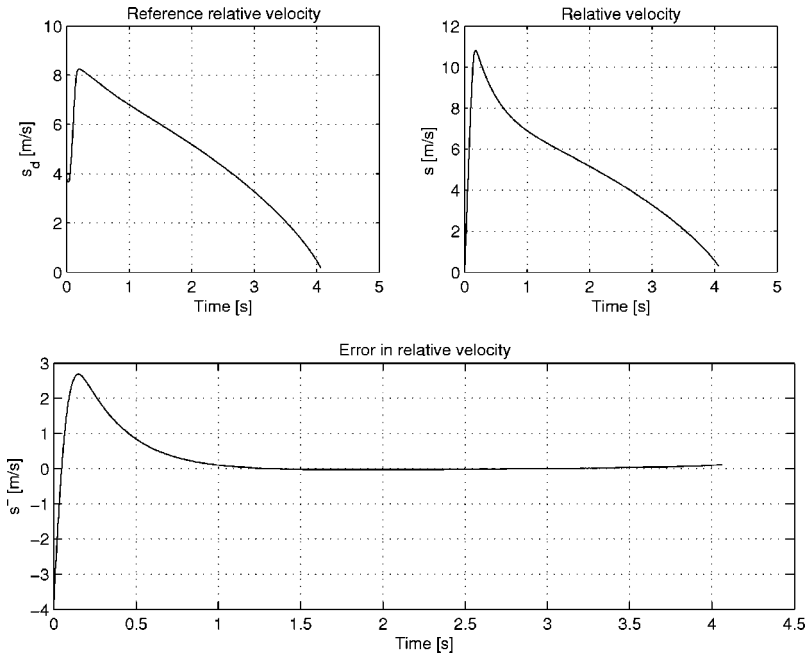

Fig. 10 Dynamic surface $\tilde{s}$ with mass M changed 30% and K_b changed 10%

perspective of safe spacing policies. Simulation results showed the capability of dynamic friction models to replicate well-known pseudostatic friction models. When applied to an emergency braking maneuver, these results showed that vehicles can be stopped quickly with a near-maximum deceleration.

There are several advantages of using this controller-observer scheme. It is a useful device to improve safety during extreme driving conditions. It can be used to derive safe spacing policies that obey real road conditions. These policies can be directly implemented in automated vehicles or indirectly through driver advise in manual traffic flow. It can interact with roadside infrastructure to help traffic management control centers to adjust network capacity when there are changes in road-tire interfaces with influence on highway capacity. It is clear that in all cases the final goal is to improve overall vehicle safety levels and to increase highway capacity in real road conditions.

There are, naturally, limitations in the approach presented in this paper and additional refinements are necessary if results are to be implemented. A more realistic model for the brake system can be used; this will lead to a better control signal for the master cylinder pressure. Another issue refers to the use of a one-quarter vehicle model. Although one of such models can be set independently for each tire, there are effects in braking, as load shifting, that have to be taken into account and incorporated in this model. If this proves not to be sufficient, then a more complex vehicle model can be used. Although the measurement of linear acceleration was included to overcome the problem of lack of observability of vehicle velocity from wheel-speed measurements, it would be convenient to add other sensors that will add robustness in the estimation of longitudinal velocity. GPS or DGPS sensors can be used for this purpose, although there are still bandwith limitations in these devices that need to be addressed.

Acknowledgments

L. Alvarez and L. Olmos thank the finantial support of UNAM-DGAPA under Grant No. PAPIIT IN-104700. J. Yi and R. Horowitz thank the support of the California PATH Program under Grant No. UCB-ITS PATH MOU-373.

References

[1] Alvarez, L., and Horowitz., R., 1999, "Safe Platooning in AHS, Part I: Safety Regions Design," Veh. Syst. Dyn. **32**(1), pp. 23–56.

[2] Carbaugh, J., Godbole, D. N., and Sengupta, R., 1997, "Tools for Safety Analysis of Vehicle Automation Systems," in *Proc. of American Control Conference*, Vol. **3**, pp. 2041–2045.

[3] Choi, W., and Swaroop, D., 2001, "Assessing the Benefits of Coordination in Automatically Controlled Vehicles," in *2001 IEEE Intelligent Transportation Systems Proc.*, pp. 72–77.

[4] Lygeros, J., Godbole, D. N., and Broucke, M. E., 2000, "A Fault Tolerant Control Architecture for Automated Highway Systems," IEEE Trans. Control Syst. Technol. **8**, pp. 205–219.

[5] Bakker, E., Nyborg, L., and Pacejka, H. B., 1987, "Tyre Modelling for Use in Vehicle Dynamic Studies," Society of Automotive Engineers Paper No. 870421.

[6] Kiencke, U., 1993, "Realtime Estimation of Adhesion Characteristic Between Tyres and Road, in *Proc., 3rd IFAC Workshop on Advances in Automotive Control*, Karlsruhe, Pergamon Press, London, pp. 101–106.

[7] Yi, J., Alvarez, L., and Horowitz, R., 2002 "Adaptive Emergency Braking Control With Underestimation of Friction Coefficient," IEEE Trans. Control Syst. Technol. **10**, pp. 381–392.

[8] Canudas de Wit, C., Olsson, H., Åstrom, K. J., and Lischinsky, P., 1995, "A New Model for Control of Systems With Friction, IEEE Trans. Autom. Control **40**(3), pp. 419–425.

[9] Canudas de Wit, C., and Tsiotras, P., 1999, "Dynamic Tire Friction Models for Vehicle Traction Control," in *Proc. of 38th IEEE Conference of Decision and Control*, Phoenix, Vol. 4, pp. 3746–3751.

[10] Canudas de Wit, C., and Horowitz, R., 1999, "Observers for Tire/Road Contact Friction using only wheel angular velocity information, in *Proc. of 38th IEEE Conference of Decision and Control*, Phoenix, IEEE, New York, pp. 3932–3937.

[11] Yi, J., Alvarez, L., Horowitz, R., and Claeys, X., 2003, "Emergency Braking Control With an Observed-Based Dynamic Tire/Road Friction Model and Wheel Angular Velocity Measurement," Veh. Syst. Dyn. **39**(2), pp. 81–97.

[12] Claeys, X., Yi, J., Alvarez, L., Horowitz, R., and Canudas, C., 2001, "A New 3-D Dynamic Tire/Road Friction Model for Vehicle Control and Simulation," in *2001 IEEE Intelligent Transportation Systems Proc.*, IEEE, New York, pp. 485–490.

[13] Deur, J., 2001, "Modeling and Analysis of Longitudinal Tire Dynamics Based on the Lugre Friction Model," in *Proc., 12th IFAC World Congress of Automatic Control*, Sydney, Pergamon Press, London, Vol. 1, pp. 15–22.

[14] Wong, J. Y., 1993, *Theory of Ground Vehicles*, 2nd Edition, Wiley, New York.

[15] J. C., Gerdes, and K. J., Hedrick, 1995, "Brake System Requirements for Platooning on an Automated Highway," in *The American Control Conference*, Seattle, WA, pp. 165–169.

[16] Yi, J., Alvarez, L., Horowitz, R., and Canudas, C., 2000, "Adaptive Emergency Braking Control Based on a Tire/Road Friction Dynamic Model," in *Proc. of 2000 Conference on Decision and Control*, IEEE, New York, pp. 456–461.

[17] Khalil, H. K., 1996, *Nonlinear Systems*, 2nd Edition, Prentice Hall, NJ.

[18] Schuring, D. J., 1976, Tire Parameter Determination. DOT HS-802 089, Calspan Corporation.

[19] F., Gustafsson, 1997, "Slip-Based Tire-Road Friction Estimation," Automatica, **33**(6), pp. 1087–1099.

[20] Burckhardt, M., 1987, *ABS und ASR, Sicherheitsrelevantes, Radschlupf-Regel System. Lecture Scriptum*, University of Braunschweig, Germany.